MODELING CREEP DEFORMATIONS OF FRP-REINFORCED GLULAM BEAMS

William G. Davids
Assistant Professor

Habib J. Dagher
Professor of Civil and Environmental Engineering
Director, Advanced Engineered Wood Composites Center

and

Joseph M. Breton
Former Graduate Research Assistant
Department of Civil and Environmental Engineering
University of Maine
Orono, ME 04469-5711

(Received September 1999)

ABSTRACT

This study focuses on the development and calibration of a numerical method for modeling creep deformations of glulam beams strengthened on the tension side with fiber-reinforced polymers (FRP). The results of an experimental investigation on the creep of twelve, 7-m-long FRP-reinforced Douglas-fir and western hemlock glulam beams are briefly presented. The experiments, conducted in a sheltered environment with controlled temperature and uncontrolled relative humidity, demonstrate that, although FRP-reinforced beams can support significantly larger loads than unreinforced beams, they do not exhibit increased relative creep. A numerical model based on layered moment-curvature analysis is developed, and a general solution strategy is detailed that permits the easy inclusion of nonlinear viscoelastic or viscoplastic material properties. A viscoelastic constitutive model is proposed for the wood that accounts for experimentally observed mechano-sorptive creep effects, and is implemented within the framework of the proposed numerical scheme. The model parameters are fitted to the unreinforced specimen test results, and the model is then shown to accurately predict the observed relative creep displacements of the reinforced specimens. Parametric studies are conducted that clearly demonstrate the effectiveness of FRP tensile reinforcing in reducing creep deformations in glulam beams.

Keywords: FRP-reinforced glulam, viscoelasticity, mechano-sorptive creep, layered analysis.

INTRODUCTION

A number of studies conducted over the past five decades have examined the effect of tensile reinforcing on the bending strength of wood. Researchers have studied the short-term effects of the addition of fiber-reinforced polymers (FRP) to the underside of both solid-sawn wood beams (Plevris and Triantafillou 1992; Abdel-Magid et al. 1994) and glulam beams (Tingley and Leichti 1993; Kimball 1995; Dagher et al. 1996; 1998). Plevris and Triantafillou (1992) found that the addition of 1.4% carbon FRP increased the bending strength of a solid wood beam by 40%. Dagher et al. (1998) reported that the allowable bending strength of glulam beams made with L2 and L3 laminations in a random lay-up increased by up to 61% with the addition of 1.1% E-glass FRP (GFRP) and by up to 119% with the addition of 3.3% GFRP, and the bending stiffness increased by up to 17%. All of these researchers concluded that the addition of FRP could force a ductile failure precipitated by compressive yielding and wrinkling of the wood.

The changing availability of forest resourc-

Wood and Fiber Science, 32(4), 2000, pp. 426–441

es and resultant difficulties in procuring high-quality tension laminations continue to spark further research in this area. One critical issue that deserves further exploration is the creep deformation of FRP-reinforced glulams, particularly since FRP reinforcement allows the use of higher design stresses. Relatively little work has been conducted on predicting the creep response of FRP-reinforced glulams. Indeed, the only related study of which the authors are aware is that of Plevris and Triantafillou (1995), who performed 10-month tests of three FRP-reinforced, solid-sawn fir beams, and implemented the viscoelastic model of Fridley et al. (1992) in an effort to develop a predictive creep model. However, Plevris and Triantafillou (1995) did not calibrate the model to their experimental results, and their experiments did not consider mechano-sorptive effects, nor the use of structural-size glulam beams.

This study addresses the development and calibration of general modeling techniques to allow the effect of different structural configuration, reinforcing ratios, and material properties on the creep deformations of FRP-reinforced glulam to be examined. Following a brief review of creep in wood structures, a long-term experimental study on creep deformations of FRP-reinforced glulams conducted by the authors is briefly reviewed. A general creep prediction model that relies on a strain-based, layered moment-curvature analysis that permits the easy inclusion of nonlinear, viscoelastic material models is then developed. A uniaxial, viscoelastic material model that incorporates mechano-sorptive effects is developed. The model parameters are calibrated to the experimental results for the unreinforced beams, and the model is then shown to accurately predict the experimentally measured creep response of the reinforced specimens. Parametric studies are conducted to examine the effect of FRP reinforcing on creep deformations. Finally, conclusions and recommendations for future research are presented.

CREEP IN STRUCTURAL TIMBER

Creep in wood is generally divided into three phases (Bodig and Jayne 1993): primary, secondary, and tertiary. At service loads, after creep progresses through the primary stage, secondary creep—characterized by a constant but reduced creep rate—continues throughout the life of the structure (Bodig and Jayne 1993). Tertiary creep, which is defined by rapidly increasing creep rates up until creep rupture, is not a consideration for the sustained compressive stress levels in the beams of this study, although it is of importance for the sustained tensile stresses experienced by the specimens in this study.

Several environmental factors can influence creep deformations of wood, including both temperature (Morlier and Palka 1994) and moisture changes (Hunt 1989). However, for the usual temperature ranges experienced by in-service structural members, moisture effects are generally more significant, and are in fact a major concern where the wood member is subjected to varying relative humidities. Water acts as a plasticizer, causing the strength and stiffness of wood to decrease as moisture content increases; the same effect produces greater creep at higher moisture contents (Bodig and Jayne 1993).

Less understood is a phenomenon known as mechano-sorptive creep, whereby a loaded member undergoing fluctuations in moisture content will creep more than a comparable member at a constant moisture content. This behavior is generally regarded as separate from viscoelastic creep, and may be of the same magnitude as the viscoelastic creep for in-service wood beams (Martensson 1994). Hunt and Shelton (1988) observed that the first moisture cycle accounts for the major part of mechano-sorptive creep, with increased creep strain during any desorption and during the first sorption at any moisture level, and decreased creep strain under future sorptions at the same moisture level. These observations have been confirmed by Ranta-Maunus (1975), Lu and Erickson (1994), Nakano

(1996), and Shen and Gupta (1997). Further, Hunt (1994) observed differing mechano-sorptive creep on the tension and compression faces of a bending member, with strains increasing rapidly in compression zones due to cell-wall buckling. Martensson and Thelandersson (1990) reported greater mechano-sorptive strain under compression as well.

To date, there has been no prior research on creep in FRP-reinforced glulam beams, although Plevris and Triantafillou (1995) performed 10-month tests of three solid-sawn fir beams 45 mm by 86 mm by 1.5 m long. The beams were loaded in 3-point bending and reinforced with carbon FRP (CFRP) laminates with reinforcement ratios of 0%, 1.18%, and 1.65%. The experimental deflection curves showed that increasing the amount of CFRP decreases both the immediate and creep deflections, with a CFRP fraction of 1.18% resulting in 40% less initial deflection and 50% less creep deflection as compared with an unreinforced beam. Plevris and Triantafillou (1995) also conducted parametric studies using the viscoelastic constitutive model for wood developed by Fridley et al. (1992) and showed that the addition of modest amounts of FRP reinforcement can substantially reduce creep deformations.

EXPERIMENTAL PROGRAM AND RESULTS

Test specimens and program

Only a brief overview of the experimental program will be presented here; for further details, see Breton (1999). A total of 12 beams—6 each of western hemlock and Douglas-fir—were loaded in 4-point bending from May 1997 to March 1999, and the central displacements were recorded with dial gages (see Fig. 1 for an illustration of the test rig). Each beam was constructed using a random lay-up of eight, 38 mm × 130 mm wood laminations of a special L2/L3 grade (Dagher et al. 1998) as shown in Fig. 1. The FRP reinforcement consisted of 0, 1, or 3 additional layer(s) of 3.2-mm-thick pultruded phenolic/E-glass FRP (GFRP) with an elastic modulus of 43,500 MPa (Dagher et al. 1998). These reinforcement levels correspond to 0%, 1.1%, and 3.3% reinforcing, respectively, based on the area of wood above the GFRP. The GFRP was sandwiched between the bottom two wood laminations; the bottom lamination—termed a "bumper lamina"—was included for aesthetic purposes and to provide protection to the FRP layer.

For the remainder of this manuscript, we will focus on the Douglas-fir specimens, the characteristics of which are provided in Table 1; note that two specimens of each reinforcing ratio were tested. The magnitudes of the total load applied to each beam shown in Table 1 were selected to produce 125% of the allowable design stress calculated in accordance with the glulam design procedure of ASTM D3737 (1996). This sustained load level is prescribed by the 1998 ASTM Draft Specification for Evaluation of Duration of Load and Creep Effects on Wood Products (ASTM 1998). Note that the stresses in Table 1 are the extreme fiber bending stresses in the wood computed from a transformed section analysis.

The experiments were performed in a structural testing facility at the University of Maine. Dehumidifiers were used to maintain relative humidities (RH) between approximately 30% and 90%, and ambient temperatures were kept between 18°C and 24°C from the start of the study until June 1998, at which time all environmental controls were removed. Figure 2 presents the average relative humidities and temperatures recorded throughout the tests. In addition to deflections, the weights of 130-mm × 305-mm × 250-mm-long Douglas-fir glulam blocks with unsealed ends were recorded daily to provide average moisture content data.

Displacement response

The individual total deflection vs. time curves for the 6 Douglas-fir beams are given in Fig. 3. For both species, the reinforced beams all experienced more total deflection than the unreinforced beams, which is expect-

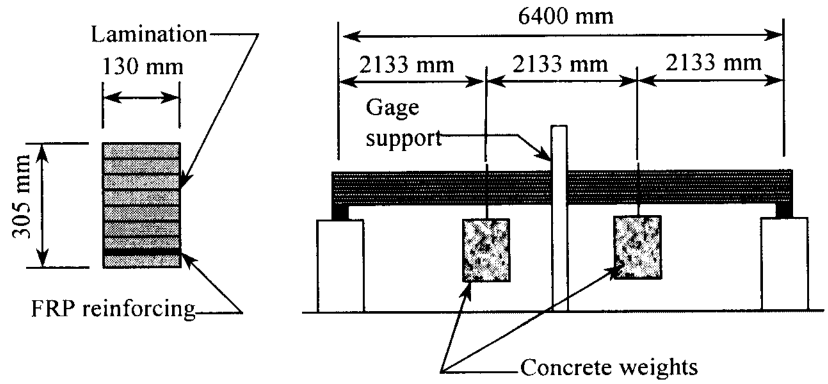

(a) Beam Cross-section (b) Creep test set-up

FIG. 1. Details of test specimen and set-up.

ed since the addition of FRP has a much greater effect on strength than on stiffness. The average initial elastic deflection of the unreinforced Douglas-fir beams was 33 mm, while that of the Douglas-fir beams with 3.3% GFRP was 55 mm. For the first 3 months of the testing program, creep rates decreased continuously, indicating that the twelve beams were all in the primary creep stage. The majority of the creep deflection occurred during this time, with deflections ranging from 9 mm to 23 mm. The deflections then increased by an average of only 8 mm for the remaining 19 months. Although the creep deflection rates increased over the winter of 1997–1998, the rates stabilized near zero after 10 months of testing.

After 5 months of testing, specimen DF-3.3%-2 experienced creep-rupture in the sacrificial wood bumper lamina. The failure was characterized by the development of a vertical crack through the bumper lamina, followed by

TABLE 1. *Test specimen designations and loads.*

FRP Ratio	Specimen Identifier	Applied Load (kN)	Applied Stress[1] (MPa)
0%	DF-0%-1	25.0 kN	13.4
	DF-0%-2		
1%	DF-1.1%-1	29.8 kN	15.9
	DF-1.1%-2		
3%	DF-3.3%-1	44.9 kN	23.3
	DF-3.3%-2		

[1] 1.25*allowable design stress on the extreme wood fiber.

an interlaminar failure of the FRP near the FRP-bumper lamina bond line. Finally, there was partial peeling of the FRP layer from the bumper lamina. No bond failure occurred between the FRP layer and the lamina directly above the FRP. This failure progression indicates that the wood-FRP bond was stronger than the interlaminar strength of the FRP, and is consistent with the failures observed in the short-term ultimate strength tests (Dagher et al. 1998). Currently, the beams are still loaded, and a detailed inspection of the FRP for manufacturing defects is not possible.

While the observed bumper lamina failure is certainly not desirable and the resultant reduced beam cross section caused a sudden increase in both elastic deflection and creep rates, the creep rates decreased again and reached a value close to zero about 5 months following the bumper lamina failure. We emphasize that the beam was able to sustain the applied loads for the duration of the creep study, and the bumper lamina failure presents a serviceability—rather than an ultimate strength—problem. Further, the ASTM Draft Specification for Evaluation of Duration of Load and Creep Effects on Wood Products (ASTM 1998) requires a 3-month test, and within this period, no failure was observed in the beam.

Since the initial elastic deflection, δ_{el}, can

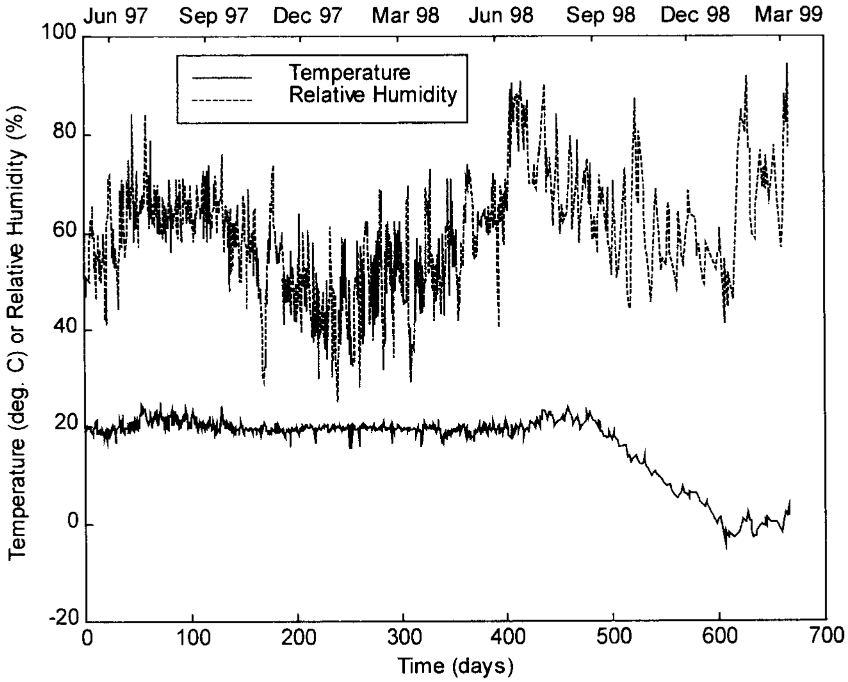

FIG. 2. Average recorded temperature and relative humidity.

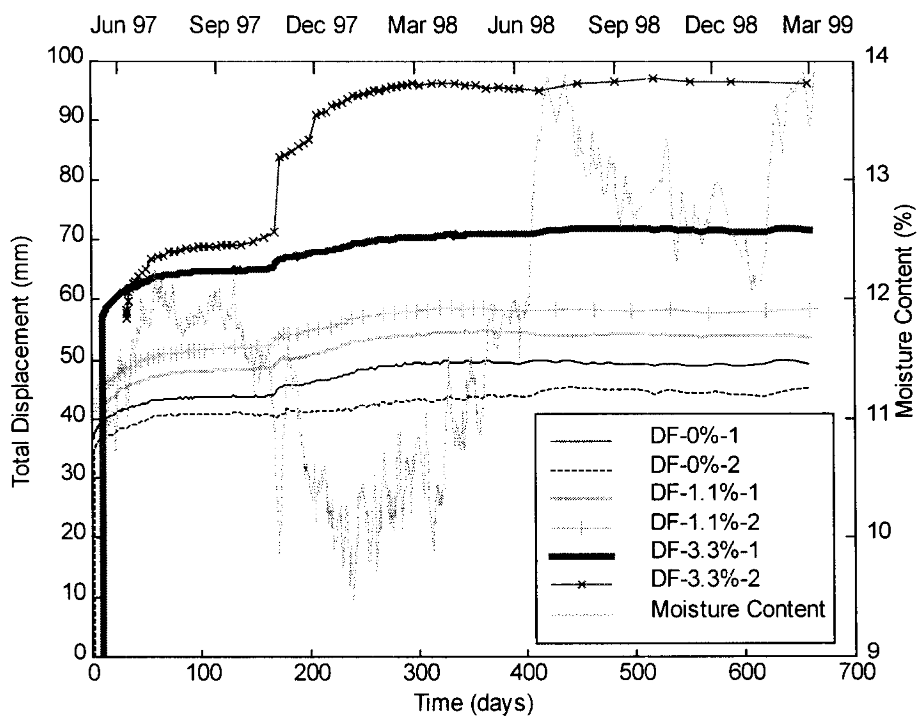

FIG. 3. Total displacement of the Douglas-fir specimens.

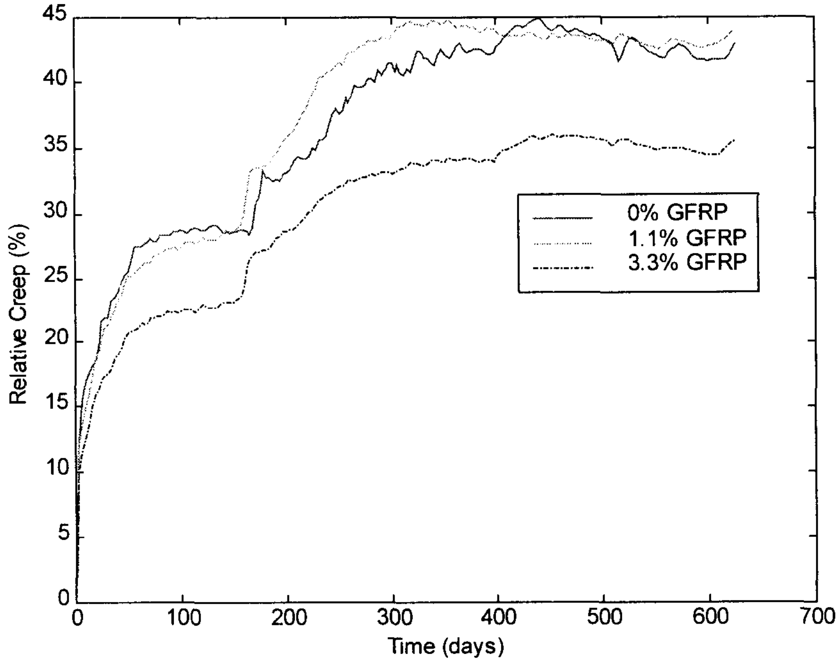

FIG. 4. Average relative creep of the Douglas-fir specimens.

change greatly depending on wood properties, lay-up, geometry, loading, and environmental conditions, it is often difficult to compare creep deflection data curves from different test specimens. Relative creep (*RC*) is often used to normalize the data sets as defined in Eq. (1), where δ_{el} is the initial elastic displacement.

$$RC = \frac{\delta_{cr}}{\delta_{el}} \times 100\% \qquad (1)$$

Figure 4 shows average relative creep—excluding the beam with the creep-ruptured bumper lamina—for each matched pair of specimens. Although the data set was limited to two repetitions for each category, there appears to be no significant difference in relative creep between the controls and the 1.1% reinforced beams, while the 3.3% reinforced beam appears to have the lowest relative creep ratio. These results are significant, indicating that even over the large range of stress levels in this study, creep deformation appears to increase linearly with sustained stress level. In other words, relative creep deformation appears to be relatively insensitive to the stress levels used in this study.

Moisture effects

Figure 3 shows that during a 2-week period in October 1997, the moisture content of the weighed blocks dropped a full 2% and then increased to its previous level. This moisture content fluctuation corresponded to the start of the heating season and caused a dramatic increase in creep deflection rates for all beams. Since the creep rates diminished after this sharp change, this increase in creep rates was not an indication of tertiary creep but is best attributed to mechano-sorptive effects. From October 1997 to February 1998 the space was heated, and the moisture content dropped from about 12% to 9.5%. During this period, all beams showed a greater creep rate than was observed in the 3 months prior to the heating season.

Once the environmental controls were deactivated in June 1998, the moisture content increased by 2%. Figure 3 shows that the creep deflection rates increased slightly with this moisture change for 4 of the 6 Douglas-fir specimens, although at magnitudes much lower than observed during October 1997. For the 9 months of testing in the uncontrolled environment, the increase in creep deflections was nearly zero despite the continuing moisture content changes. This indicates that the mechano-sorptive creep may have become exhausted after enough moisture cycles (Hunt 1989) for the observed range of moisture content. Most of the beams showed negligible response to the high adsorption rates of June 1998 and January 1999.

NUMERICAL MODELING OF CREEP RESPONSE

The focus of this section is the development of a numerical model to permit the prediction of the creep response of FRP-reinforced wood beams having different reinforcement ratios, cross-sectional geometries, and subjected to arbitrary loadings. First, we present the motivation for, and development of, a simple uniaxial constitutive model for wood that captures the mechano-sorptive effects observed in the laboratory specimens. Next, a general time-stepping procedure for the solution of the viscoelastic differential equations in each wood layer that makes no assumptions with regard to linearity—and does not employ superposition—is proposed. Note that the GFRP reinforcement used in this study was subjected to sustained stress levels of less than 15% of its mean ultimate strength; at these levels of stress, the creep deformations in GFRP are negligible compared to those in the wood and can be safely ignored. The layered moment-curvature analysis performed at regularly spaced intervals along the beam to yield the time-dependent curvatures is also discussed.

Uniaxial viscoelastic model for wood

Numerous models for the prediction of the uniaxial time-dependent response of wood can be found in the literature. Early investigations employed a simple power law (Schniewind 1968) which has the disadvantage of being applicable to only constant load histories (Hoyle et al. 1985). In response to this deficiency, the well-known Burger body was developed (Senft and Suddarth 1971), which consists of serial Kelvin and Maxwell viscoelastic elements (see Fig. 5). However, a Burger body with constant coefficients cannot capture variations in creep arising from moisture, temperature, and mechano-sorptive effects.

Many investigators have since developed more sophisticated models that attempt to capture environmental effects on the creep response of wood. Fridley et al. (1992) developed a creep model based on a Burger body that incorporates mechano-sorptive creep effects as well as moisture and temperature-dependent variations in stiffness. Mohager and Toratti (1993) presented a mechano-sorptive model encompassing different tensile and compressive compliance functions. In addition to a linear creep model, a combined model incorporating partially irrecoverable (plastic) compressive strains was proposed. Martensson (1994) developed yet another viscoelastic model that decomposed strain rate into elastic, viscoelastic, shrinkage-swelling, and creep components. More recently, Lu and Leicester (1997) presented a mechano-sorptive model coupled with a simple approximate solution for moisture variation within a specimen based on Fick's law of diffusion and sinusoidal fluctuations in ambient moisture boundary conditions.

Despite the efforts of various investigators to develop a comprehensive approach to predicting the creep of wood, independent applications of the various models found in the literature are relatively rare. One exception is the model of Fridley et al. (1992), which Plevris and Triantafillou (1995) implemented in a study on the creep response of FRP-reinforced solid-sawn wood beams that was designed to evaluate the effectiveness of different FRP types. However, the environmental conditions assumed in the analyses were hypothetical, and the three laboratory specimens tested by Plevris and Triantafillou (1995) were not subjected to temperature and humidity variations.

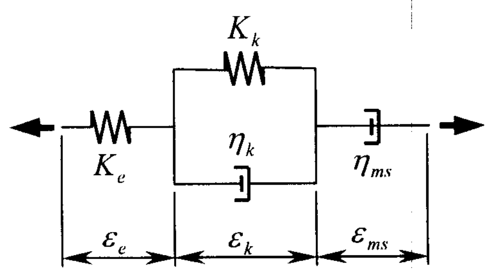

FIG. 5. Viscoelastic constitutive model.

Shen and Gupta (1997) utilized the model of Fridley et al. (1992) for comparison with their experimental data on 2 × 4 Douglas-fir beams subjected to 4-point loading and cyclic temperature and humidity conditions, and found relatively poor agreement with their experimental results. Shen and Gupta (1997) developed a simpler model based on a four-element Burger body that yielded somewhat better predictions, and concluded that the mechano-sorptive element in Fridley's model was not sensitive to the relatively small humidity changes of their test program.

The laboratory results presented previously (see Figs. 2–4) indicate that mechano-sorptive effects are significant for the specimens of the present study. In contrast, the relatively small ranges of moisture and temperature variation experienced by the specimens likely did not produce significant variations in material properties of the timber (Bodig and Jayne 1993). Thus, we have chosen to use a straightforward uniaxial model for the wood as shown in Fig. 5, which incorporates mechano-sorptive effects through a dashpot with properties dependent on the time rate of change of moisture content.

The governing equations for this uniaxial system can be written as follows, where stress is expressed as a function of strain and strain rate for the individual model elements:

$$\sigma = K_e \epsilon_e \tag{2}$$

$$\sigma = \eta_k \dot{\epsilon}_k + K_k \epsilon_k \tag{3}$$

$$\sigma = \eta_{ms} \dot{\epsilon}_{ms} \tag{4}$$

$$\epsilon = \epsilon_e + \epsilon_k + \epsilon_{ms} \tag{5}$$

In Eqs. (2)–(5), σ denotes stress, and the individual strain components (ϵ_e, ϵ_k, ϵ_{ms}) are as defined in Fig. 5. An overdot defines the time rate of change of strain. The constant K_e represents the elastic modulus of the wood; K_k and η_k comprise a viscoelastic Kelvin element; and η_{ms} is the mechano-sorptive creep coefficient. While many investigators choose to represent strain as a function of stress, most structural analyses are based on stiffness methods that employ the convention of Eqs. (2)–(5); this facilitates use of the general solution technique discussed later in this section.

To capture increasing creep with high rates of moisture content change, the mechano-sorptive creep coefficient, η_{ms}, is inversely related to the absolute value of the time rate of change of moisture content, $|\dot{u}|$, by

$$\eta_{ms} = \frac{\eta'_{ms}}{|\dot{u}|} \tag{6}$$

where η'_{ms} is a model parameter, and assumed to be a material constant. As noted by several investigators (Ranta-Maunus 1975; Hunt and Shelton 1988; Bazant 1985; Martensson 1994; Lu and Erickson 1994), the first cycle of wetting and drying produces the largest mechano-sorptive creep effects, with subsequent wetting cycles causing no or even reduced creep deformations. Further, prior research has indicated the presence of a mechano-sorptive creep limit, beyond which mechano-sorptive creep is negligible (Hunt 1989).

Estimating the presence of such a limit for the specimens of this accelerated study is difficult because of the small number of global fluctuations in moisture, upon which are superimposed higher frequency fluctuations that also appear to contribute to mechano-sorptive creep. However, Figs. 3 and 4 clearly show that for all specimens, there is a large increase in creep coinciding with the first drying cycle, with a sharp jump in creep rates occurring at about day 170 corresponding to a sharp drop in moisture content. Further, both unreinforced specimens exhibit a moderate increase in creep rates from days 370–440, which corresponds to the region where the moisture contents of the second wetting cycle exceed the maximum moisture content previously experienced by the specimens. To capture these effects in the present model, η'_{ms} is considered constant throughout the first wetting and drying cycles, and mechano-sorptive creep is included for subsequent moisture cycles only when the moisture content falls within the maximum and minimum values previously experienced by the specimen.

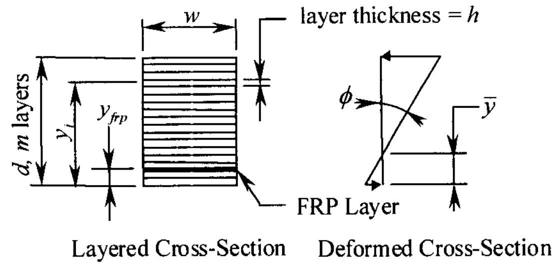

FIG. 6. Geometry and variables for layered section analysis.

Solution of the viscoelastic equations

A general numerical, time-stepping approach has been adopted for the solution of Eqs. (2)–(5) that is both compatible with conventional stiffness-based structural analysis methods and permits the easy inclusion of moisture, temperature, and nonlinear stress- or strain-dependent material properties.

The size of the system of coupled ordinary differential equations given in Eqs. (2)–(5) can be reduced by substituting Eq. (2) into Eqs. (3) and (4), and solving for $\dot{\epsilon}_{ms}$ and $\dot{\epsilon}_k$ in terms of ϵ_e. Solving Eq. (5) for ϵ_e and substituting the results into the remaining expressions yields:

$$\dot{\epsilon}_{ms} = \frac{K_e}{\eta_{ms}}(\epsilon - \epsilon_k - \epsilon_{ms}) \tag{7}$$

$$\dot{\epsilon}_k = \frac{K_e}{\eta_k}(\epsilon - \epsilon_k - \epsilon_{ms}) - \frac{K_k}{\eta_k}\epsilon_k \tag{8}$$

Equations (7) and (8) are a pair of coupled ordinary differential equations written in terms of component strains; all terms are as defined previously for Eqs. (2)–(5). Many techniques are available for the solution of this system, including the explicit Euler's method as well as various implicit methods. For the present simulations, the implicit trapezoidal rule was chosen for the solution due to its second-order accuracy and unconditional stability. Further, in lieu of integrating a compliance function over the entire time-history at each time step—which can lead to significant computational expense—only the data from the previous and current time steps are needed at each point in the iteration. We emphasize that no assumptions have been made with regard to linearity, and superposition has not been employed.

Layered analysis and nonlinear solution strategy

The layered moment-curvature analysis method presented here is straightforward and has been used in several investigations of the time-dependent response of wood beams (Mohager and Toratti 1993; Lu and Leicester 1997) and is common in the analysis of reinforced concrete structures (Lin and Burns 1981). A typical beam cross section is shown in Fig. 6.

Denoting the externally applied moment and axial force as M and P, respectively, we can write the vector of external forces as $\mathbf{F} = [P\ M]^T$, where T denotes a transpose; $P = 0$ in the present case. Similarly, the vector of internal forces is defined as $\mathbf{F}' = [P'\ M']^T$, where P' denotes the internal axial force ($P' = 0$ in the present case), and M' is the internal moment. P' and M' are computed according to:

$$P' = \sum_{i=1}^{m} \sigma_i hw + \sigma_{frp}A_{frp} \tag{9}$$

$$M' = \sum_{i=1}^{m} (\sigma_i hw)y_i + \sigma_{frp}A_{frp}y_{frp} \tag{10}$$

In Eqs. (9) and (10), σ_{frp} and A_{frp} refer to the FRP tensile stress and area, respectively, and

y_{frp} is the distance from the bottom of the beam to the center of the FRP layer. The ith wood layer is located a distance y_i from the bottom of the beam and experiences a uniaxial stress of σ_i. The dimension h is the thickness of an individual wood layer, and w is the cross-sectional width of the beam. In general, the cross section can be divided into m equal-thickness wood layers; preliminary convergence studies indicated that $m = 20$ gives sufficiently accurate results. See Fig. 6 for further clarification of terms.

Equilibrium requires that at each time step, the following vector equation be satisfied:

$$\mathbf{F} - \mathbf{F}' = \mathbf{0} \tag{11}$$

The stress in a wood layer at any time t^{n+1} can be computed from Eqs. (2)–(5) given the strain components at time t^n and the current strain ϵ_i^{n+1}, which is a function of the distance to the neutral axis, $\bar{y}$, and the curvature, ϕ (see Fig. 6). The usual assumption of plane bending sections (Gere and Timoshenko 1984) ensures that compatibility between layers is enforced. Equation (11) is then seen to represent a system of two nonlinear equations with two unknowns, $\bar{y}$ and ϕ, and is solved at each time step with an implementation of Newton's method that relies on a finite difference approximation to the Jacobian. Preliminary studies showed that 20 layers were sufficient to give convergent results.

While a simpler analysis method and solution strategy (i.e. a transformed section method with a compliance based equivalent elastic modulus) could be used with the proposed rheological model, the more general techniques presented here will easily permit the consideration of more sophisticated nonlinear material models and complex geometries in future studies.

COMPARISON OF EXPERIMENTAL AND ANALYTICAL RESULTS

The previously described viscoelastic constitutive model and solution strategy have been implemented using the commercially available scientific and engineering analysis package Matlab ("Using Matlab"), and used to predict the creep response of the University of Maine Douglas-fir beams. This section details the parameter estimation and compares the experimental and predicted results.

Parameter estimation

Estimation of the unknown constitutive parameters K_e, K_k, η_k, and η'_{ms} for the unreinforced beams was achieved through the following procedure:

1) The relative creep data for the two unreinforced Douglas-fir beams (see Fig. 4) were averaged and smoothed by sampling at 100 unequally spaced time intervals that accurately captured the displacement response.
2) The measured moisture content was fitted with a seventh-order polynomial to capture the low frequency components of the variation in moisture content as shown in Fig. 7.
3) The elastic modulus, K_e, was computed based on the initial elastic deflection as 11,530 MPa.
4) Initial estimates for K_k and η_k of 26,700 MPa and 320,000 MPa·day, respectively, were taken from the study of Fridley et al. (1992) based on tests of 71 2×4 Douglas-fir bending specimens. Preliminary analyses indicated that the model results were relatively insensitive to the value of η_k, and it was fixed at 320,000 MPa·day.
5) The values of K_k and η'_{ms} were determined that provided the best least-squares fit to the measured data. This was accomplished through use of the simplex-based multivariate minimization routine `fmins()` available in Matlab ("Using Matlab"). The assumed starting values were K_k = 26,700 MPa and η'_{ms} = 320,000 MPa·day per % change in moisture content, and the optimal values were determined to be K_k = 55,000 MPa and η'_{ms} = 200,000 MPa·day^2 per % change in moisture content.

Figure 8 shows both the predicted and average measured responses over 650 days of

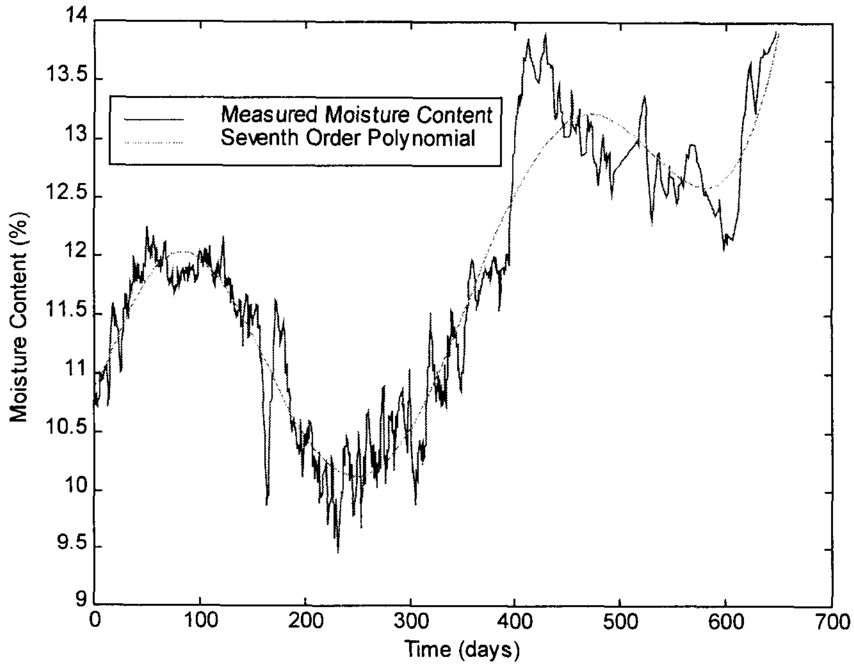

FIG. 7. Measured and fitted moisture content for Douglas-fir specimens.

loading for the unreinforced Douglas-fir beams. In general, the model predictions are good, capturing the observed increases in deformation corresponding to rapid moisture content changes. Note that the model predicts two distinct regions of increased creep for the intermediate drying/wetting cycle, slightly underpredicting mechano-sorptive creep for the first drying cycle between days 100 and 250, and overpredicting for the subsequent portion of the wetting cycle where moisture contents are in excess of the previous maximum value of 12% reached at about day 100. A possible explanation for this is the contribution of the many smaller, high-frequency drying/wetting cycles to mechano-sorptive creep experienced by the specimen that are not captured by the model. Overall, however, the total relative creep occurring throughout the specimen load history is captured with good accuracy.

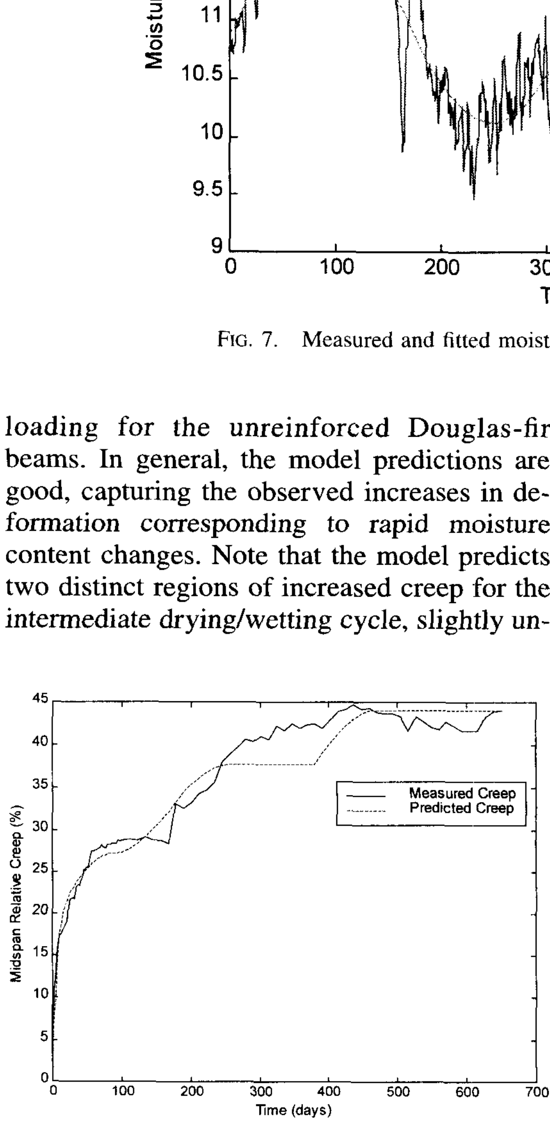

FIG. 8. Predicted and measured relative creep of Douglas-fir beams with 0% reinforcing.

To validate the model, it was then used to predict the response of the Douglas-fir beams reinforced with 1.1% and 3.3% FRP using the previously determined parameters. Figure 9 compares the average measured and predicted response for specimens DF-1.1%-1 and DF-1.1%-2. In contrast to the unreinforced specimens, these beams exhibited a gradually reduced creep rate over the entire period from 170–350 days, followed by a slight reduction in creep. The model again predicts two more

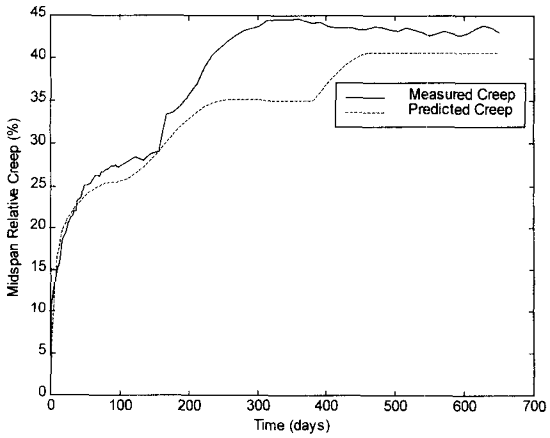

FIG. 9. Predicted and measured relative creep of Douglas-fir beams with 1.1% reinforcing.

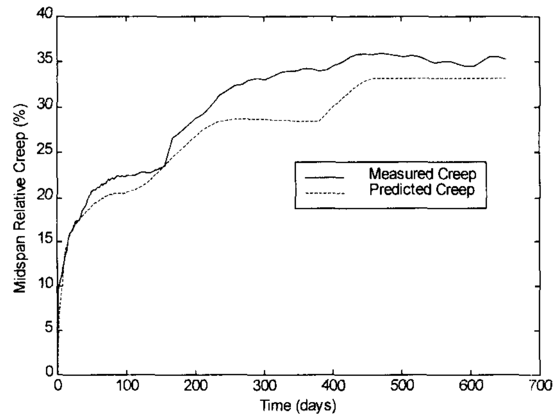

FIG. 10. Predicted and measured relative creep of specimen DF-3.3%-1.

marked regions of increased creep over the same time frame, with a maximum error in the predicted creep of 20% at about day 360; however, the total predicted creep deformation at the end of the 650 days of testing is remarkably accurate.

Figure 10 shows the measured and predicted creep response of only specimen DF-3.3%-1, since specimen DF-3.3%-2 suffered a creep rupture failure of the bumper lumina. For this beam, we observe a good correlation between the experimental and numerical results over the full time frame of the test, picking up the observed increase in creep with both the drying and wetting cycles. Again, the total creep displacement at the end of the testing period is predicted quite well.

EFFECT OF FRP REINFORCEMENT ON CREEP DEFORMATIONS

While the laboratory tests indicate that the relative creep of FRP-reinforced glulams is not larger than that of unreinforced glulams, the effectiveness of FRP-reinforcing on reducing creep cannot be inferred from the test data due to the different load levels. In this section, simulations employing the calibrated numerical model are used to examine the effect of FRP-reinforcing on reducing creep. In addition to creep deformations, the change in stress in the FRP-reinforcing with time is quantified.

The same geometric configuration illustrated in Fig. 1 is used for the parametric studies, with the total applied load fixed at 12.5 kN—the value used in the experiments for the unreinforced beams. Two types of reinforcing are employed: a unidirectional GFRP with E = 43,500 MPa, and a unidirectional carbon fiber-reinforced polymer (CFRP) with E = 182,000 MPa. Reinforcement ratios of 0%, 1.1%, and 3.3% are considered for both the GFRP and CFRP specimens. The material properties for the timber laminations remain unchanged from the values determined during calibration to the experimental results, and the same environmental conditions observed during the physical testing program are employed.

Figure 11 shows the midspan relative creep vs. time for the six beams. Two immediate conclusions can be drawn from Fig. 11:

1) The volume fraction of the FRP has a significant effect on reducing creep deformations, with 1.1% GFRP reducing relative creep by 10%, and 3.3% GFRP reducing relative creep deformations by 26%.
2) The GFRP stiffness also significantly affects creep, with 1.1% CFRP being nearly as effective at reducing creep as 3.3% GFRP.

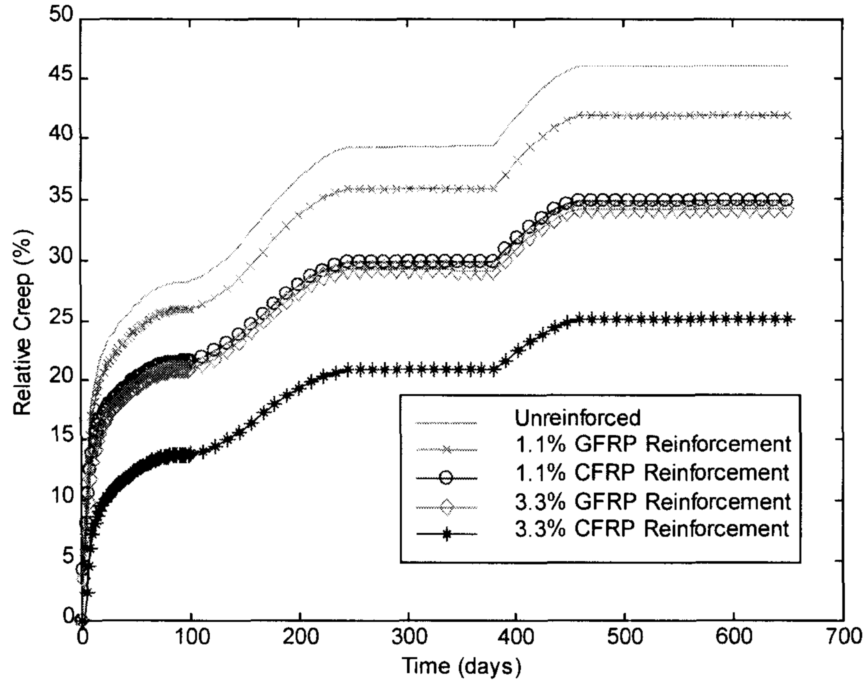

FIG. 11. Effect of FRP type and reinforcement ratio on relative creep.

While properly reinforced FRP-reinforced glulam is known to have larger flexural strength and ductility than unreinforced glulam (Kimball 1995; Dagher et al. 1998), the conclusions reached here indicate that another practical application for these hybrid members may be the reduction of creep deformations in members with large sustained dead loads such as bridges.

Figure 12 illustrates the effect of creep on the tensile stresses in the FRP. As expected, for specimens with either GFRP or CFRP, increasing the reinforcement ratio decreases the initial FRP stresses. For the same applied load, the CFRP experiences a 43% reduction in stress as the reinforcement ratio is increased from 1.1% to 3.3%, while the GFRP sees a smaller reduction of 17% due to its lower elastic modulus. However, creep in the wood increases the tensile stresses in the FRP, with the maximum change occurring in the 1.1% GFRP which sees a 43% increase in tensile stress over the 650-day simulation period. It must be noted that continued creep will further increase these stresses, and estimation of the maximum FRP tensile stress over an actual structure's lifetime would require realistic consideration of all mechano-sorptive, temperature, and moisture-induced creep effects. Along with durability of the FRP and the long-term FRP-wood bond strength, this is a design issue that warrants further study. In all cases, however, the final tensile stress levels (after 650 days) are quite low: the 1.1% GFRP specimen sees at most 7% of its mean ultimate tensile strength of 731 MPa, and the CFRP is also stressed to only a small fraction of its ultimate tensile capacity.

SUMMARY AND CONCLUSIONS

The results of a long-term experimental study on creep deformations in FRP-reinforced glulam beams were overviewed. Twelve specimens laminated from Douglas-fir and western hemlock and reinforced on the tension side with uniaxial E-glass fiber-reinforced polymer (GFRP) were tested for over

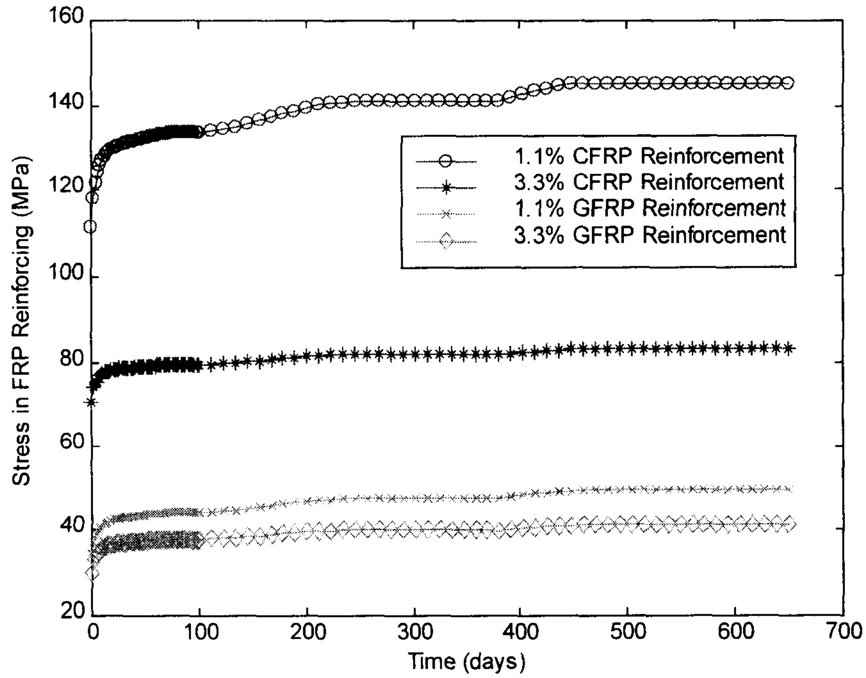

FIG. 12. Tensile stress in FRP as a function of time.

650 days under 4-point bending in a sheltered environment. Humidity, temperature, and moisture content were monitored in addition to the center-span displacement. When compared to the unreinforced specimens, the reinforced beams did not exhibit increased relative creep displacements despite their higher loading.

A numerical procedure for simulating creep deformations in FRP-reinforced glulams was developed that is based on a layer moment-curvature analysis. The adopted stiffness-based procedure is very general, relying on a direct solution of the governing system of ordinary differential equations at each time step. This approach has several advantages:

1) Superposition is not assumed, and more sophisticated, nonlinear material models can be incorporated with relative ease.
2) The costly integration of a compliance function over the full time-history at each time step is avoided; only the strain components at the previous and current time steps need be known.
3) The version of Newton's method employed in the equilibrium iteration can be used with various geometric configurations and materials with little difficulty.

A viscoelastic model was proposed for wood that incorporates mechano-sportive effects and strain-dependent shrinkage and swelling. The viscoelastic model parameters were back-calculated based on the displacements of the unreinforced specimens, and the model was used in simulations of the creep response of the reinforced Douglas-fir beams. The model accurately predicted the experimentally observed creep deformations for the beams having both 1.1% and 3.3% GFRP reinforcing, especially in light of the small sample size, the inherent variability of wood, and the averaging of the measured moisture content data taken from separate specimens with unsealed ends.

A parametric study was conducted with the validated numerical model to examine the effectiveness of FRP tensile reinforcing at reducing creep deformations in glulam beams.

Both GFRP and carbon fiber-reinforced polymer (CFRP) materials were considered as reinforcement. The simulation showed that FRP can reduce creep deformations significantly, with 3.3% GFRP reducing creep deformations over 26% for environmental conditions and specimens similar to those of this study. A smaller amount of CFRP—only 1.1%—is nearly as effective at reducing creep as 3.3% GFRP due to its higher modulus of elasticity. The tensile stresses in the FRP were shown to increase with creep deformations, although they remained at a small fraction of their ultimate tensile strength. However, the tensile stress increase at the lower reinforcement ratios is significant. For the 1.1% GFRP reinforcement, the stress in the GFRP increased by 43% over the 650-day simulation period.

Future work is planned at the University of Maine on the creep response of FRP-reinforced glulam and timber beams. In addition to further long-term testing of structural-size beams under controlled environmental conditions, testing of small-scale specimens subjected to the high uniaxial compressive stresses common to FRP-reinforced beams is planned. These experimental studies will be supplemented with the development of more sophisticated constitutive models and numerical techniques that capture the coupled moisture transport/stress-strain response of FRP-reinforced timber subjected to realistic environmental exposure conditions.

REFERENCES

ABDEL-MAGID, B., H. J. DAGHER, AND T. KIMBALL. 1994. The effect of composite reinforcement on structural wood. Proc. ASCE Materials Engineering Conf. Infrastructure: New Material and Methods for Repair, November 14–16, San Diego, CA.

AMERICAN SOCIETY FOR TESTING AND MATERIALS (ASTM). 1996. Standard practice for structural glued laminated timber (glulam). ASTM D3737-93c. American Society for Testing and Materials, Philadelphia, PA.

———, 1998. Draft specification for evaluation of duration of load and creep effects of wood products. American Society for Testing and Materials. Philadelphia, PA.

BAZANT, Z. P. 1985. Constitutive equation of wood at variable humidity and temperature. Wood Sci. Technol. 19: 159–177.

BODIG, J., AND B. A. JAYNE. 1993. Mechanics of wood and wood composites. Krieger Publ. Co., Malabar, Fl.

BRETON, J. M. 1999. Creep behavior of FPR-reinforced Douglas-fir and western hemlock glulam beams. M.S. thesis, Dept. of Civil and Environmental Engineering, University of Maine, Orono, ME.

DAGHER, H. J., T. E. KIMBALL, AND S. M. SHALER. 1996. Effect of FPR-reinforcement on low grade eastern hemlock glulam. Proc. National Conf. On Wood Transportation Structures, October 23–25, Madison, WI.

———, B. ABDEL-MAGID, R. LINDYBERG, J. POULIN, AND S. SHALER. 1998. Static bending test results of Douglas-fir and western hemlock FPR-reinforced glulam beams. AEWC Rept. No. 98-4, University of Maine, Orono, ME.

FRIDLEY, K. J., R. C. TANG, AND L. A. SOLTIS. 1992. Creep behavior model for structural lumber. J. Struct. Eng. 118(8):2261–2277.

GERE, J. M., AND S. P. TIMOSHENKO. 1984. Mechanics of materials, 2nd ed. PWS Publishers, Boston, MA.

HOYLE, R. J., M. C. GRIFFITH, AND R. Y. ITANI. 1985. Primary creep of Douglas-fir beams of commercial size and quality. Wood Fiber Sci. 17(3):300–314.

HUNT, D. G. 1989. Linearity and non-linearity in mechano-sorptive creep of softwood in compression and bending. Wood Sci. Technol. 23:323–333.

———, 1994. Present knowledge of mechano-sorptive creep of wood. RILEM Rept. 8, E. and F. N. Spon, London, UK.

———, AND C. F. SHELTON. 1988. Longitudinal moisture-shrinkage coefficients of softwood at the mechano-sorptive creep limit. Wood Sci. Technol. 22:199–210.

KIMBALL, T. 1995. Feasibility of glulam beams reinforced with FPR sheets. M.S. thesis, Dept. Civil and Environmental Engineering University of Maine, Orono, ME.

LIN, T. YL, AND N. H. BURNS. 1981. Design of prestressed concrete structures. John Wiley and Sons, New York, NY.

LU, J. P., AND R. H. LEICESTER. 1997. Mechano-sorptive effects on timber creep. Wood Sci. Technol. 31:331–337.

LU, W., AND R. ERICKSON. 1994. The effects of directed diffusion on the mechano-sorptive behavior of small redwood beams. Forest Prod. J. 44(1):8–14.

MARTENSON, A. 1994. Creep behavior of structural timber under varying humidity conditions. J. Struct. Eng. 120(9):2565–2582.

———, AND S. THELANDERSSON. 1990. Effect of moisture and mechanical loading on wood materials. Wood Sci. Technol. 24:247–261.

MOHAGER, S., AND T. TORATTI. 1993. Long term bending creep of wood in cyclic relative humidity. Wood Sci. Technol. 27:49–59.

MORLIER, P., AND L. C. PALKA. 1994. Basic knowledge of creep in timber structures. Pages 9–42 *in* RILEM Rept. 8, E. and F. N. Spon, London, UK.

NAKANO, T. 1996. Viscosity and entropy change in creep during water desorption for wood. Wood Sci. Technol. 30(2):117–125.

PLEVRIS, N. AND T. TRIANTAFILLOU. 1992. FPR-reinforced wood as structural material. J. Mater. Civil Eng. 4(3): 300-317.

———, AND ———. 1995. Creep behavior of FPR-reinforced wood members. J. Struct. Eng. 121(2):174–186.

RANTA-MAUNUS, A. 1975. The viscoelasticity of wood at varying moisture content. Wood Sci. Technol. 9:189–205.

SCHNIEWIND, A. P. 1968. Recent progress in the study of the rheology of wood. Wood Sci. Technol. 2:188–206.

SENFT, J. F., AND S. K. SUDDARTH. 1971. An analysis of creep-inducing stress in Sitka spruce. Wood Fiber 2(4): 321–327.

SHEN, Y., AND R. GUPTA. 1997. Evaluation of creep behavior of structural lumber in a natural environment. Forest Prod. J. 47(1):89–96.

TINGLEY, D. A., AND R. J. LEICHTI. 1993. Reinforced glulam: Improved wood utilization and product performance. Paper presented at Globalization of Wood: Supply Products and Markets, Forest Prod. Soc., Portland, OR.

USING MATLAB. 1998. The Mathworks, Inc., Natick, MA.